Scientific paper

Study on Impact Response of Reactive Powder Concrete Beam and Its Analytical Model

Kazunori Fujikake[1], Takanori Senga[2], Nobuhito Ueda[3], Tomonori Ohno[4] and Makoto Katagiri[5]

Received 27 June 2005, accepted 3 November 2005

Abstract

The aim of this study was to experimentally examine the impact response of a RPC (Reactive Powder Concrete) beam and develop an analytical model to represent its impact response. Thus, a drop hammer impact test was performed to investigate the influence of drop height of the hammer on the impact response of the RPC beam. Subsequently, a static flexural loading test was conducted to find out the residual load carrying capacity of the RPC beam after impact loading. In the impact analysis, the two degrees of freedom mass-spring-damper system model was used. The analytical results were in good agreement with the experimental results when high damping for the local response at the contact point was assumed.

1. Introduction

Reactive Powder Concrete (RPC) reinforced with short steel fibers is characterized by an ultra-high strength of more than 200 MPa and high fracture toughness. Because of its excellent properties, RPC may be suitable as an advanced material for reinforced concrete structures subjected to impact loads resulting from crashing vehicles, ships or airplanes, falling rocks, avalanches or explosions. However, since RPC is a relatively new material, little information on the impact response of RPC is available. The current state of the art concerning impact responses of reinforced concrete members is limited to normal strength concrete (JSCE 1993, Norwegian Defence Construction Service 1996, JSCE 2004). Therefore, it is essential to investigate the impact response of RPC and to provide an analytical model to represent its response.

Impact loading is generally an extremely severe loading condition characterized by great intensity and short duration. The behavior of a structural member under impact loading may consist of two responses; one is the local response mainly due to the stress wave that occurs at the loading point during a very short period after impact, and the other is the overall response with vibration effects due to the elastic-plastic deformation that occurs in the whole structural member over a long period after impact. The overall response strongly depends on the quasi-static behavior with loading rate effect of the structural member. It is well known that the rapid loading test is the best way to examine the quasi-static behavior of a structural member under constant high deformation velocity.

The authors have already conducted a number of studies, outlined below, concerning the dynamic mechanical characteristics of RPC for the purpose of collecting fundamental data required for better understanding and modeling the impact behaviors of RPC beams. The uniaxial tensile and the triaxial compression behaviors of RPC under rapid loading were examined and constitutive models with strain-rate effects for RPC were proposed (Fujikake *et al*. 2002, Fujikake *et al*. 2006a). The rapid flexural behaviors of RPC beams were investigated with experimental variables consisting of the rate of loading and the amount of longitudinal tension rebar, and an analytical model based on a fiber model technique was finally developed to predict the quasi-static behavior of reinforced RPC beams subjected to rapid flexural loads (Ueda *et al*. 2005, Fujikake *et al*. 2006b).

The aim of this study was to experimentally examine the impact response of a RPC beam and to develop an analytical model to represent its impact response. Thus, two kinds of test were performed. One was a drop hammer impact test to evaluate the impact response of the RPC beam, and the other was a static flexural loading test to find out the residual load carrying capacity of the RPC beam after impact loading.

2. Experimental program

2.1 Test specimens

Five identical RPC beams with an I section were prepared for the impact loading test. The RPC beams had the cross-sectional dimensions of 200 mm depth, 150 mm width, and 1700 mm length, as shown in **Figs. 1** and **2**. The RPC beams were provided with three deformed bars

[1]Associate Professor, Department of Civil and Environmental Engineering, National Defense Academy, Japan.
E-mail: fujikake@nda.ac.jp
[2]Officer, Ground Self-Defense Force, Japan.
[3]Research Engineer, Research & Development Center of Taiheiyo Cement Corporation, Japan.
[4]Professor, Department of Civil and Environmental Engineering, National Defense Academy, Japan.
[5]Manager, Research & Development Center of Taiheiyo Cement Corporation, Japan.

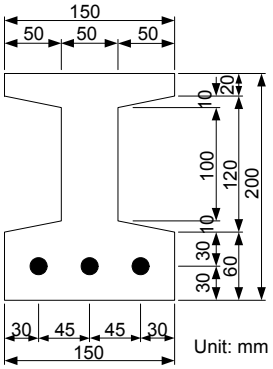

Fig. 1 RPC beam cross section detail.

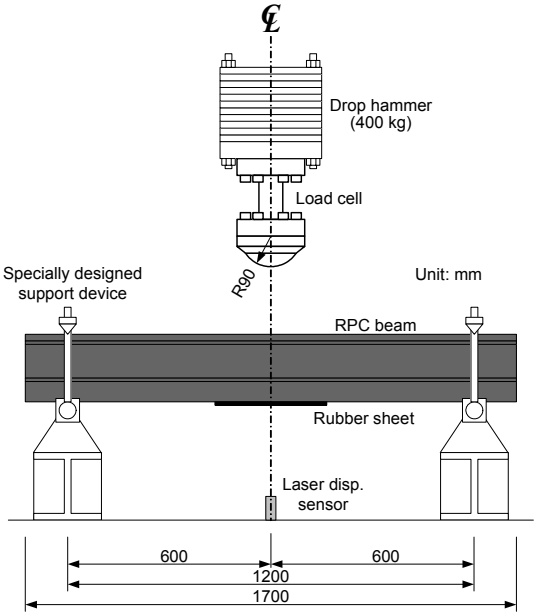

Fig. 2 Drop hammer impact test setup.

with a diameter of 13 mm, as shown in **Fig. 1**. An effective depth of 170 mm was maintained for the longitudinal reinforcement. The reinforcement ratio was 2.60%. The RPC beams tested were identical to the specimens that were used in our previous rapid flexural loading test, in which the specimens had exhibited a type of ductile flexural failure (Ueda *et al*. 2005).

2.2 Material compositions and properties

Table 1 details the mix proportions used in this study. The pre-blended powders, provided as Ductal Premix on a commercial basis, consist of Portland cement, silica fume, quartz sand with a maximum particle diameter of 1.2 mm used as fine aggregate and very fine powder composed mainly of quartz as the mineral admixture. Two percents of short straight steel fibers in volume were introduced to the mix. The steel fibers used were 15 mm long, with a diameter of 0.2 mm. After their removal from the molds, all specimens were cured at 90℃ for 2 days. The mechanical properties of RPC used in uniaxial static compression tests are given in **Table 2**. The mild steel reinforcement used for longitudinal reinforcement had a yield strength of 295 MPa and an elastic modulus of 200 GPa.

Table 1 Mix proportions.

Fiber volume fraction V_f (%)	2.0
Water-cement ratio W/C (%)	22.0
Water*1 (kg/m^3)	180
Pre-blended powders [Ductal] (kg/m^3)	2254
Steel fiber (kg/m^3)	157
Superplasticizer (kg/m^3)	25

*1 including superplasticizer

Table 2 Mechanical properties of RPC under static loading.

Compressive strength	214.7 MPa
Flexural strength	40.0 MPa
Young's modulus	55 GPa
Poisson ratio	0.2

2.3 Impact loading test

For impact loading, a drop hammer impact loading machine was used, as shown in **Fig. 2**. A drop hammer with a mass of 400 kg was dropped freely onto the top surface of the RPC beam at midspan from five different heights: 0.8, 1.0, 1.2, 1.4 and 1.6 m. The striking tup had a hemispherical tip with a radius of 90 mm. To prevent the RPC beam from bouncing out, the RPC beam was supported over a span of 1200 mm with specially designed devices allowing it to freely rotate.

The contact force developed between the hammer and the RPC beam was measured using a dynamic load cell. The midspan deflection response of the RPC beam was measured using a displacement laser sensor as well. The dynamic load cell was rigidly connected to the drop hammer. A thin rubber sheet was mounted on the bottom surface of the RPC beam as a target for the laser sensor, so that the midspan deflection could be measured after cracking. The PC-based data acquisition system recorded the data at a sampling rate of 100 kHz.

2.4 Residual load carrying capacity test

The residual load carrying capacity of the RPC beam after impact loading was examined using a static flexural loading test. In the test, the RPC beam was simply supported over a span of 1200 mm, and loaded at midspan at the midspan deflection rate of 1.4×10^{-4} m/s. The acting load and the midspan deflection were measured using a load cell and a displacement laser sensor, respectively.

3. Experimental results

3.1 Failure modes

Typical failure modes obtained in the impact loading test are shown in **Fig. 3**. While no shear reinforcement was provided to the RPC beams in this study, no shear failure

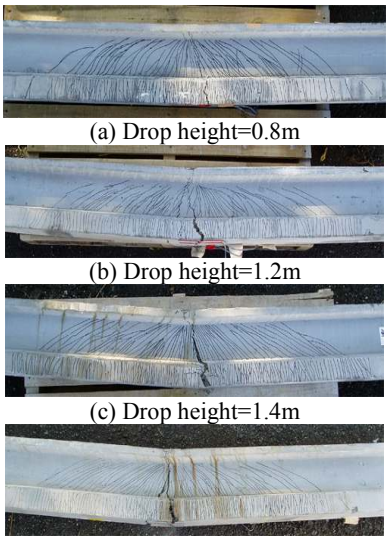

(a) Drop height=0.8m

(b) Drop height=1.2m

(c) Drop height=1.4m

(d) Drop height=1.6m

Fig. 3 Failure modes under impact loading.

was observed at all. Every specimen exhibited a type of ductile flexural tension failure with numerous fine cracks called multiple cracks, which is the same failure mode as that obtained under rapid flexural loading (Ueda *et al*. 2005). Multiple cracks are characteristic of the RPC beam subjected to flexural loading, and cannot be observed in ordinary reinforced concrete beam. The length of the multiple cracking region of the RPC beam was approximately 110 cm regardless of the drop heights of the hammer, while the crack opening of the major crack formed at midspan increased with increases in drop height. Note that no fracture of reinforcing steel was observed.

3.2 Influence of drop height on impact load-midspan deflection relation

Figure 4 shows the impact load-midspan deflection relation obtained at each drop height. The impact load-midspan deflection relations show two peaks in the midspan deflection range of less than 10 mm and an extremely steep leading edge of the initial peak, while the impact load tends to be largely constant at midspan deflections greater than 10 mm. It can be seen that the maximum midspan deflection increases with increases in drop height. In the impact test, after the main impact response shown in **Fig. 4**, the separation and contact behaviors between the hammer and the RPC beam were monitored over several times.

3.3 Residual load carrying capacity of RPC beam

Figure 4 also shows the load-midspan deflection relation obtained in the residual load carrying capacity test. In the figure, the load-midspan deflection relations obtained from both the impact loading test and the static flexural loading test for a virgin specimen done by Ueda *et al*. (2005) before the impact loading test, are also plotted for reference purposes. The load-midspan deflection relations obtained in the residual load carrying capacity test can be seen to be in good agreement with that of the virgin specimen under static loading. This evidence suggests that the impact loading does not induce any extra overall flexural damage to the RPC beam other than the overall flexural damage corresponding to the maximum deformational response. Therefore, regardless of the loading type, such as static or impact, the degree of

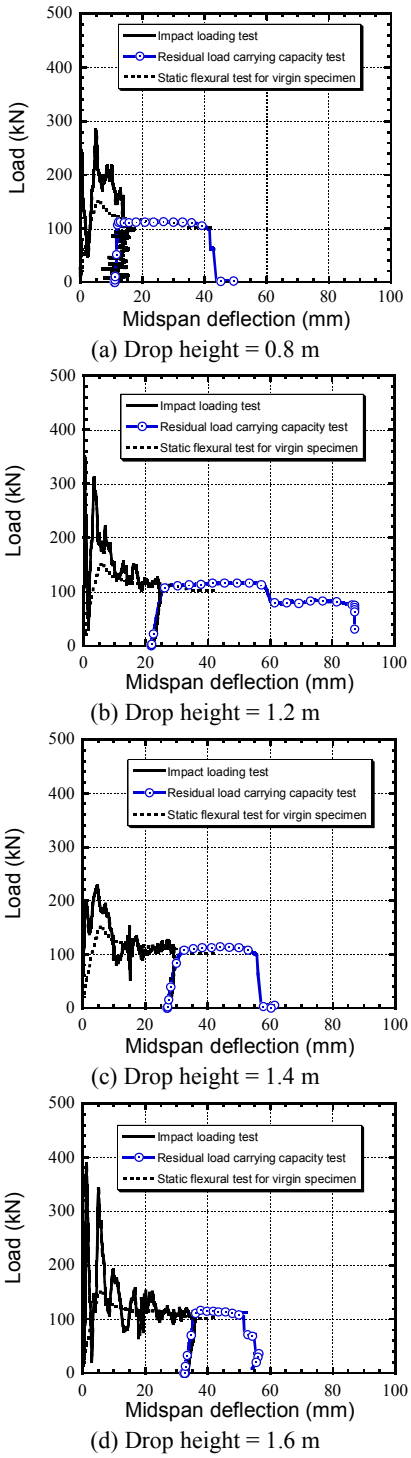

(a) Drop height = 0.8 m

(b) Drop height = 1.2 m

(c) Drop height = 1.4 m

(d) Drop height = 1.6 m

Fig.4 Impact loading and residual load carrying capacity test results.

overall flexural damage to the RPC beam probably depends only on the maximum deformational response, so that the maximum deformational response can be used as the most rational index for evaluating the overall flexural damage to the RPC beam.

In the residual load carrying capacity test, the RPC beams were loaded up to the complete loss of their load carrying capacities. However, in the static flexural loading test for the virgin specimen, loading was terminated when the midspan deflection was over 40 mm, even though the specimen still retained ample load carrying capacity. Thus, a straight comparison of the deformational capacity of the virgin specimen with that of the RPC beams after impact loadings is not possible.

4. Impact response analysis

4.1 General description

The response of a RPC beam subjected to a drop hammer impact may be represented by the two degrees of freedom mass-spring-damper system schematically shown in **Fig. 5**. The RPC beam is characterized by a mass M_1, a damping coefficient c_1 and a spring constant k_1. The drop hammer has a mass M_2. The local response at the contact point is described by a damping coefficient c_2 and a spring constant k_2. The equations of motion for the two degrees of freedom system can be expressed as:

$$\begin{bmatrix} M_1 & 0 \\ 0 & M_2 \end{bmatrix}\begin{Bmatrix} \ddot{u}_1 \\ \ddot{u}_2 \end{Bmatrix}+\begin{bmatrix} c_1+c_2 & -c_2 \\ -c_2 & c_2 \end{bmatrix}\begin{Bmatrix} \dot{u}_1 \\ \dot{u}_2 \end{Bmatrix}$$

$$+\begin{bmatrix} k_1+k_2 & -k_2 \\ -k_2 & k_2 \end{bmatrix}\begin{Bmatrix} u_1 \\ u_2 \end{Bmatrix}=\begin{Bmatrix} 0 \\ M_2 g \end{Bmatrix} \quad (1)$$

where g : acceleration of gravity, u_i, $\dot{u}_i$, $\ddot{u}_i$: displacement, velocity and acceleration of the mass M_i (i = 1,2).

This analytical model can represent not only the overall response of the RPC beam but also the local response at the contact point between the drop hammer and the RPC beam with the least degrees of freedom. The impact load measured using the dynamic load cell in the impact loading test corresponds to the load acting on the spring k_2 in the analytical system. In the following sections, the methods to determine the mechanical properties k_1, k_2, c_1 and c_2 are originally developed.

4.2 Load-midspan deflection relation of RPC beam

Freely dropping the hammer from the heights of 0.8 to 1.6 m causes initial impact velocities of 3.96 to 5.6 m/s [*impact velocity = (2 × gravity acceleration × drop height)*$^{1/2}$]. It is assumed that a RPC beam subjected to drop hammer impact at midspan deforms at a midspan deflection rate equal to the initial impact velocity of the hammer. The load-midspan deflection relation at the midspan deflection rates of 3.96 to 5.60 m/s can be estimated by using the previously proposed analytical model based on a fiber model technique, in which the strain-rates effects of RPC and reinforcing steel are properly considered (Fujikake *et al*. 2006b), as shown in **Fig. 6**. The material parameters used in the analysis are a static compressive strength of 214.7 MPa and an elastic modulus of 55.0 GPa for RPC, and a static yield strength of 295 MPa and an elastic modulus of 200 GPa for reinforcing steel. The analytical results are shown in **Fig. 7**. As can be seen, varying the midspan deflection rates between 3.96 and 5.60 m/s, no significant differences exist. **Table 3** shows the maximum load, ultimate load and ultimate midspan deflection obtained by the analysis at each loading rate. The ultimate state is defined as a point at which the extreme compression fiber at the cross section of the RPC beam at midspan reaches the dynamic compressive strength of RPC with strain-rate effect.

For the impact analysis, the load-midspan deflection relation at the midspan deflection rate of 4.85 m/s, which exhibited a relation that was the average of those calculated, was adopted and expressed by a five-segmentt curve as shown in **Fig. 8**. The loads and midspan deflections at points A to D in **Fig. 8** are shown in **Table 4**. The

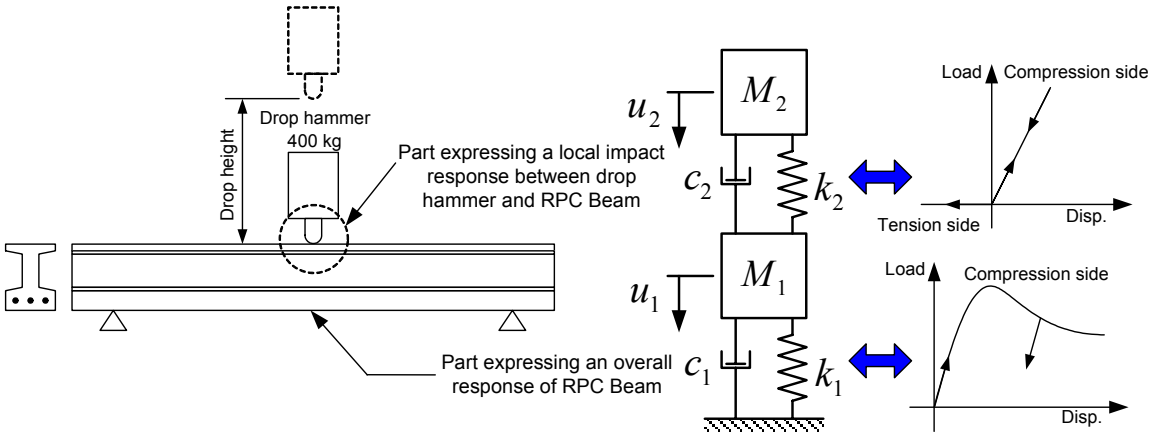

Fig. 5 Analytical model for impact loading.

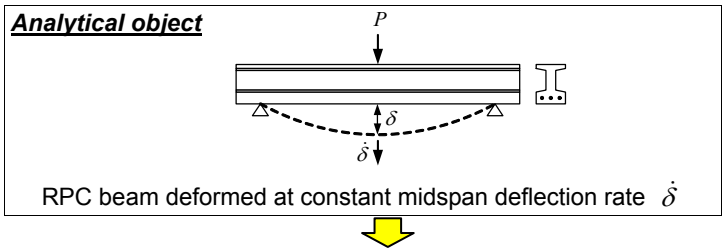

Analytical assumptions

1) Plane sections of the RPC beam before bending remain plane after bending.
2) Stress and strain within each discrete fiber element are calculated at the centroid of the fiber element.
3) Additional deformation due to shearing force is ignored.
4) A perfect bond exists between RPC and reinforcing steel.
5) The stress-strain curves with strain-rate effects for RPC and reinforcing steel are known.
6) The curvature varies with the constant curvature rate $\dot{\phi}$ given as a function of the constant midspan deflection rate $\dot{\delta}$

Analysis of moment-curvature relationship

The moment-curvature relationship is calculated based on the fiber model technique.

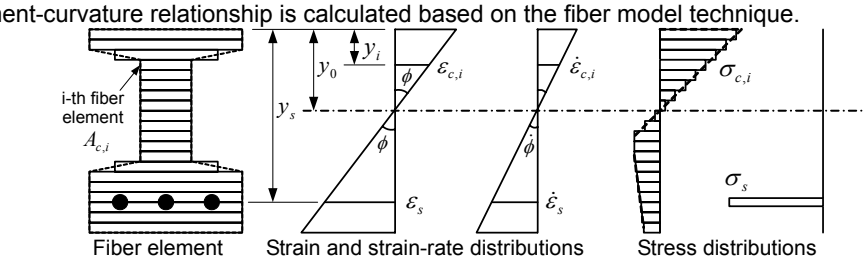

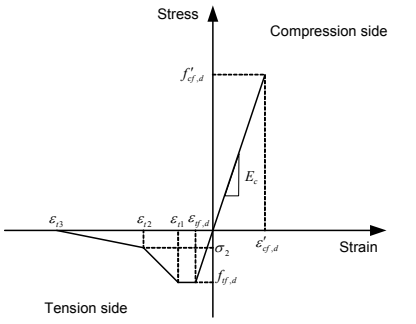

Stress-strain of RPC at strain-rate $\dot{\varepsilon}_{c,i}$

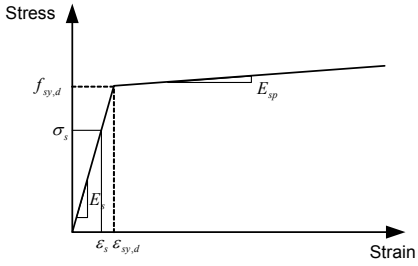

Stress-strain of reinforcing steel at strain-rate $\dot{\varepsilon}_s$

Calculation of load-midspan deflection relationship

The load-midspan deflection relationship is calculated through the moment-curvature relationship obtained.

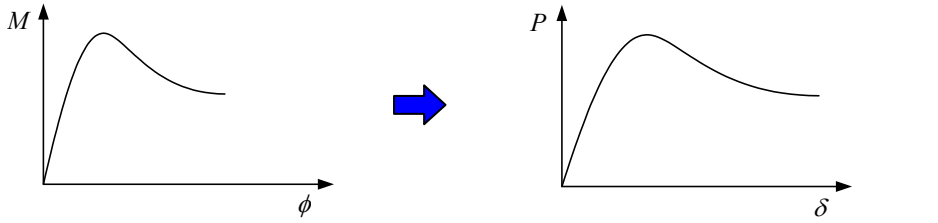

$M-\phi$ relationship at curvature rate $\dot{\phi}$ $P-\delta$ relationship at midspan deflection rate $\dot{\delta}$

Fig. 6 Analytical model to determine load-midspan de flection relation under constant midspan deflection rate $\dot{\delta}$.

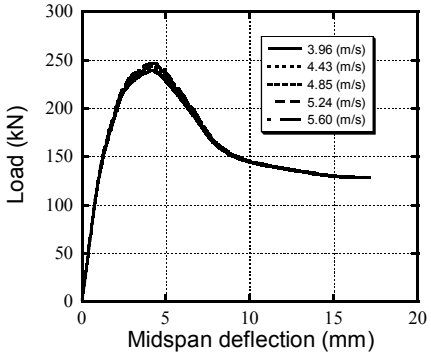

Fig. 7 Load-midspan deflection relations of RPC beam at different loading rates.

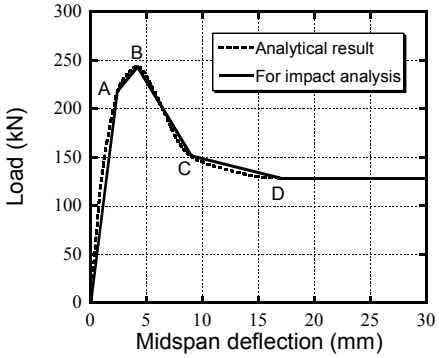

Fig. 8 Load-midspan deflection relation of RPC beam for impact analysis.

Table 3 Maximum load, ultimate load and ultimate midspan deflection at each loading rate.

Midspan deflection rate (m/sec)	Maximum load (kN)	Ultimate load (kN)	Ultimate Midspan deflection (mm)	Corresponding drop height (m)
3.96	238.77	128.17	16.8	0.8
4.43	241.30	128.36	16.9	1.0
4.85	243.40	128.52	17.0	1.2
5.24	245.23	128.67	17.1	1.4
5.60	246.83	128.79	17.1	1.6

Table 4 Detail of five-segment curve model.

Point	Load (kN)	Midspan deflection (mm)	Remarks
A	218.46	2.4	Initial rebar yielding point
B	243.40	4.2	Maximum load point
C	151.50	9.0	
D	128.52	17.0	Ultimate state point

ultimate load and the ultimate midspan deflection calculated were 128.52 kN and 17.0 mm, respectively. In the impact analysis, it was assumed that beyond the ultimate state, the load maintained the ultimate load of 128.52 kN, based on the previous research results (Ueda *et al*. 2005, Fujikake *et al*. 2006b).

4.3 Contact condition

The following conditions were employed to express the behavior of contact and separation between the drop hammer and the RPC beam:

$$\begin{cases} \text{If } (u_2 - u_1) \geq 0 \text{ then contact} \\ \text{If } (u_2 - u_1) < 0 \text{ then separation} \end{cases} \quad (2)$$

When the drop hammer and RPC beam remain in contact, the internal forces between them can be transmitted through the interface spring k_2 and the damper c_2. However when they separate, the values of both k_2 and c_2 are zero.

4.4 Interface spring

The striking tup had a hemispherical tip with a radius of 90 mm. The collision of the drop hammer and the RPC beam can be modeled as the case of contact between a spherical body and a plane, as shown in **Fig. 9**. Based on Hertz's contact theory, the relation between a local deformation δ and a contact force P can be given as (JSCE 2004):

$$P = K\delta^{3/2} \quad (3)$$

where

$$K = \frac{4\sqrt{R}}{3}\left[\frac{1-\nu_1^2}{E_1} + \frac{1-\nu_2^2}{E_2}\right]^{-1} \quad (4)$$

in which E_1, E_2 and ν_1, ν_2 are Young's moduli and Poisson's ratios of the two bodies, and R is the radius of the spherical body.

Figure 10 shows the relation between the contact force and the local deformation at the contact point in the drop hammer impact test of the RPC beam, obtained from Eq. (3) with the following mechanical properties: E_1 = 200.0 GPa, ν_1 = 0.3, E_2 = 55.0 GPa, ν_2 = 0.2. The calculated contact force-local deformation relation can be seen to be nonlinear. However, it was assumed in this analysis that the contact force-local deformation relation was linear elastic because of its simplicity.

To determine the value of interface spring constant k_2, the impact response of the RPC beam and the drop hammer were calculated varying the interface spring constant. In the calculation, the drop hammer (M_2 = 400 kg) struck on the RPC beam (M_1 = 30 kg) at midspan at a velocity of 4.85 m/s; the five-segment curve model with an initial spring constant k_{1i} = 91,000 kN/m shown in **Fig. 8** was used for the spring k_1; and the damping coefficients c_1 and c_2 were both zero. **Figure 11** shows the calculation results. The impulses or the midspan deflections are identified regardless of the interface spring constant, while the impact load increases with increases in the interface spring constant. Therefore,

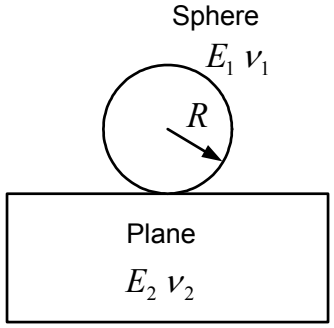

Fig. 9 Contact between sphere and plane.

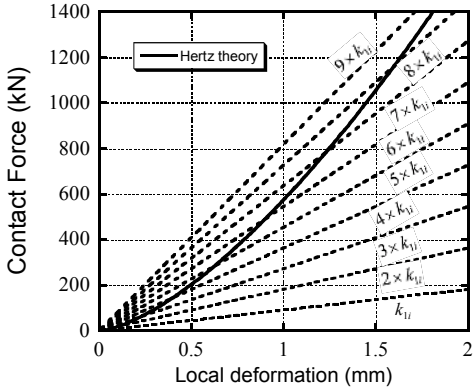

Fig. 10 Relation between contact force and displacement.

the interface spring constant should be determined taking into consideration the magnitude of the impact load.

The maximum impact loads measured were approximately 400 kN, so that the value of the interface spring was assumed to be five times larger than the initial spring constant for the RPC beam (k_{1i} = 91,000 kN/m). Thus k_2 was estimated to be 455,000 kN/m.

5. Analytical investigation

5.1 Comparison with experimental results

To check the validity of the proposed impact analysis, the impact test result obtained at the drop height of 1.2 m was selected for comparison with the analytical result. In the impact analysis, the equivalent mass of the RPC beam and the mass of the drop hammer were M_1 = 30 kg and M_2 = 400 kg, respectively. For the spring k_1 expressing the behavior of the RPC beam, the five-segment curve model shown in **Fig. 8** was used. The contact spring was k_2 = 455,000 kN/m. In the damping coefficients, five cases of damping proportional to the stiffness matrices, i.e., Rayleigh damping, were assumed, as shown in **Table 5**.

Figure 12 provides a comparison of the analytical results with the impact test results of the RPC beam. In the analytical results without damping, spike-like responses are remarkable; these analytical responses differ from the experimental response obtained. However, as the damping increases, the analytical results approach the experimental results. The analytical results of Case-5

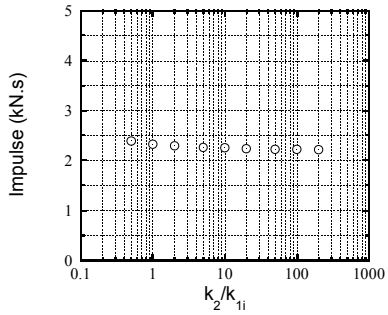

(a) Impulse

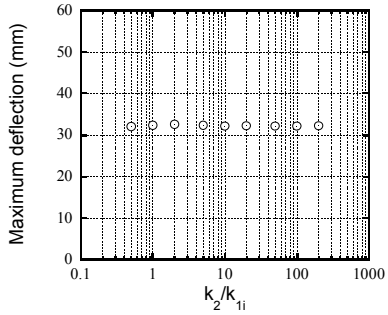

(b) Maximum deflection

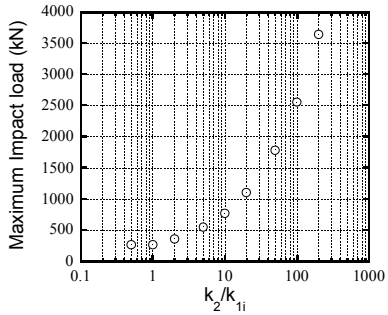

(c) Maximum impact load

Fig. 11 Influence of contact spring on analytical impact response.

Table 5 Damping used in impact analysis.

Designation	Damping coefficient		Damping constant	
	c_1 (kN.s/m)	c_2 (kN.s/m)	For 1st mode h_1	For 2nd mode h_2
Case-1	0	0	0	0
Case-2	1.0	5.0	0.002	0.024
Case-3	2.0	10.0	0.005	0.048
Case-4	4.0	20.0	0.009	0.096
Case-5	8.5	42.5	0.020	0.205

Table 6 Analytical results concerning energy.

Drop height (m)	Input energy E_I (J)	Maximum absorbed energy of RPC beam E_A (J)	Loss of energy E_L (J)	$\frac{E_A}{E_I}$
0.8	3,138.1	2,705.9	432.2	0.862
1.0	3,922.7	3,335.1	587.6	0.850
1.2	4,707.2	3,940.1	767.1	0.837
1.4	5,491.7	4,536.9	954.8	0.826
1.6	6,276.3	5,116.6	1,159.7	0.815

with c_1 = 8.5 and c_2 = 42.5 kN.s/m is basically in good agreement with the experimental results.

The analytical results using c_1 = 8.5 and c_2 = 42.5 kN.s/m for the drop heights of 0.8, 1.0, 1.4 and 1.6 m are shown in **Fig. 13** with the experimental results. The analytical results are in good agreement with the experimental results.

As shown in **Table 5**, using the damping coefficients c_1 = 8.5 and c_2 = 42.5 kN.s/m leads to a first mode damping constant of 2% and a second mode damping constant of 20.5%. Thus, in the impact analysis, the considerable degree of damping must be taken into account.

Table 6 shows the maximum absorbed energy of the RPC beam, the loss of energy and the ratio of the maximum absorbed energy of the RPC beam to the input energy obtained from the impact analysis. The relation between the maximum absorbed energy and the drop height and the relation between the ratio of the maximum absorbed energy to input energy and the drop height are shown in **Fig. 14** as well. The maximum absorbed energy of the RPC beam increases with increases in drop height, while the maximum absorbed energy approximately corresponds to 82% to 86% of the input energy. Thus, 14% to 18% of the input energy is lost.

5.2 Impact load and impulse

To examine the influence of drop height on impact load, the first peak and second peak of the impact load (shown in **Fig. 12 (e)**) obtained from both the impact test and the impact analysis were focused on, as shown in **Fig. 15**. Those peaks characterize the local response at the contact point between the drop hammer and the RPC beam from the physical phenomenon aspect. The first peaks of the impact loads obtained by the analysis increase with increases in drop height. However, those obtained from the impact test vary quite a bit. It is difficult to know whether the first peaks increase with increases in the drop height

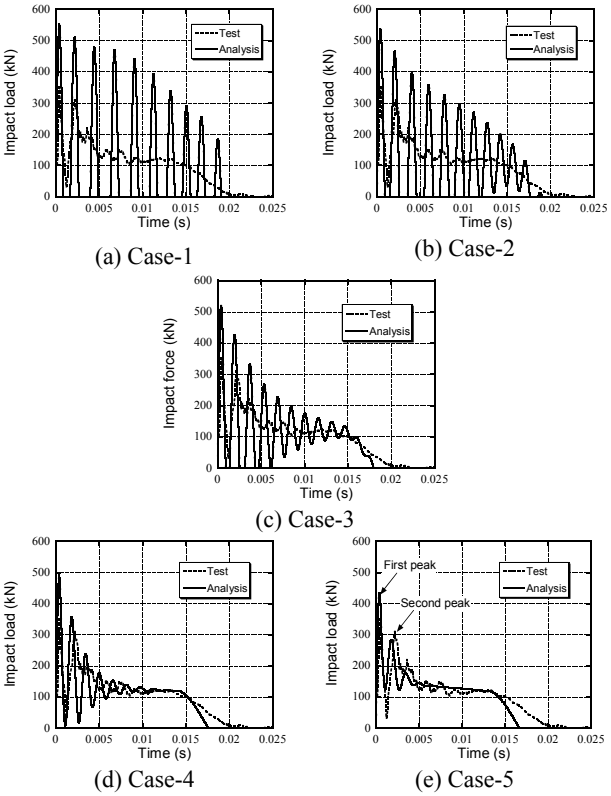

(a) Case-1 (b) Case-2

(c) Case-3

(d) Case-4 (e) Case-5

Fig. 12 Comparison of proposed analytical model with impact test result (Drop height = 1.2 m).

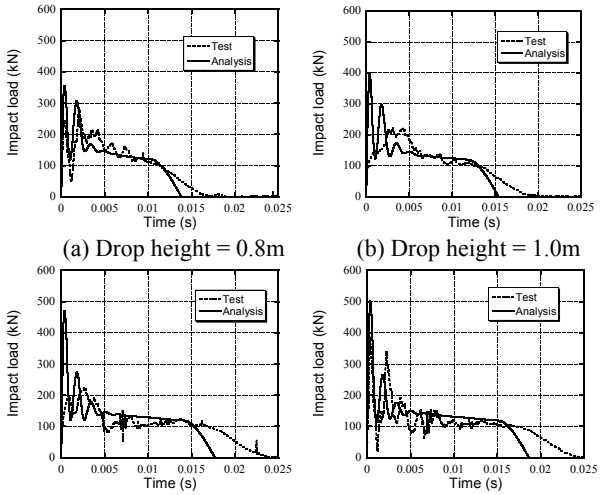

(a) Drop height = 0.8m (b) Drop height = 1.0m

(c) Drop height = 1.4m (d) Drop height = 1.6m

Fig.13 Comparison of proposed analytical model with impact test results at different drop heights.

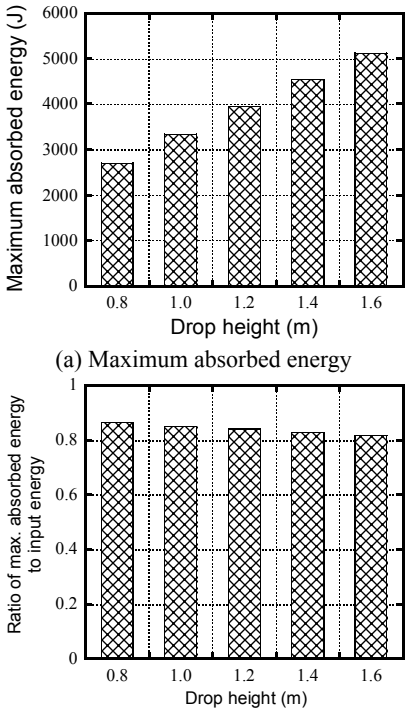

(a) Maximum absorbed energy

(b) Ratio of max. absorbed energy to input energy

Fig. 14 Maximum absorbed energy of RPC beam under impact loading.

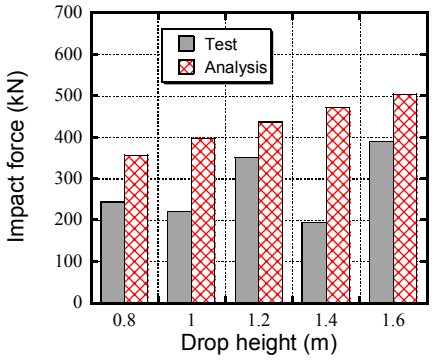

(a) First peak of impact load

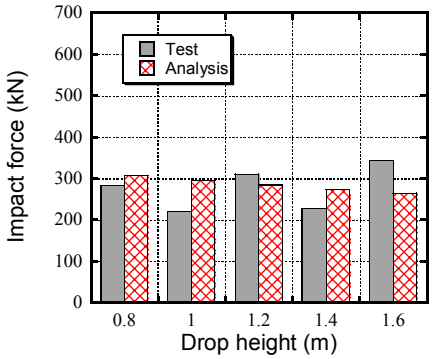

(b) Second peak of impact load

Fig. 15 First and second peaks of impact load.

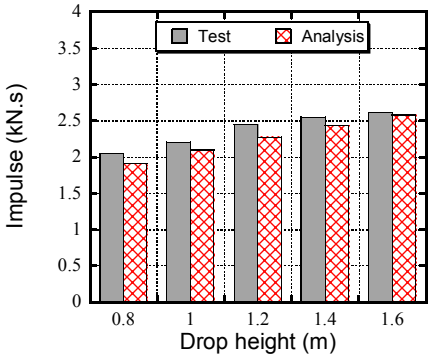

Fig. 16 Relation between impulse and drop height.

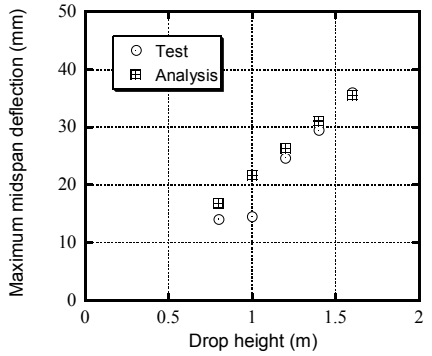

Fig. 17 Maximum midspan deflection of RPC beam under impact loading.

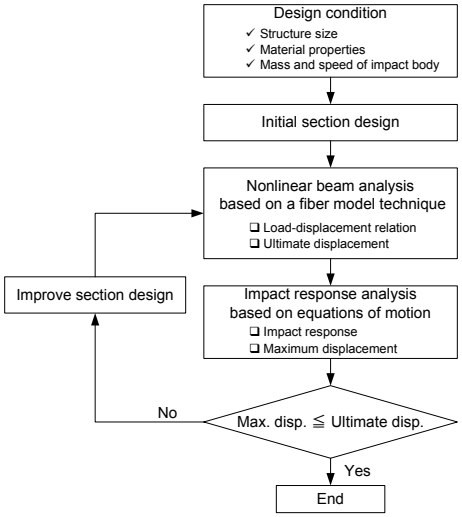

Fig. 18 Design flow of RPC beam subjected to impact loading.

or remain constant. These results suggest that it is difficult to measure the first peak of the impact load because of the degree of flatness of the contact planes and various other reasons. On the other hand, for the second peaks, the analytical values almost agree with the experimental values. The values of the second peaks almost remain constant regardless of the drop height.

Figure16 shows the relation between the impulse and the drop height obtained from the impact test and the impact analysis. The analytical impulse can be seen to be almost in agreement with the experimental one at each drop height. The impulse increases with increases in drop height.

5.3 Maximum midspan deflection of RPC beam

Figure 17 shows the relation between the maximum deformation of the RPC beam and the drop height obtained in both the impact test and the impact analysis. The analytical results are generally in good agreement with the test results, and even the analytical maximum midspan deflections at the drop heights of 0.8 and 1.0 m are larger than those obtained from the impact test.

In the previous section, test results suggested that there is a correlation between the maximum deformational response and the degree of flexural damage to the RPC beam subjected to impact loading. Therefore, the examination of structural safety for the RPC beam under impact loading is made possible by comparing the analytical maximum deformational response with the ultimate deformation as shown in **Fig. 18**, if the RPC beam only exhibits flexural failure.

Taking this impact loading test as an example, the analytical ultimate midspan deflection was estimated to be 17.0 mm. The maximum midspan deflection of the RPC beam at the drop height of 0.8 m is 16.7 mm less than the ultimate deformation, so that this case can be considered safe. On the other hand, the maximum midspan deflections at drop heights greater than 0.8 m exceed the ultimate midspan deflection, so that these

cases may be unsafe and require design changes. However, since the RPC beam for the drop height of 1.6 m showed enough residual load carrying capacity after impact loading, further research on the assessment procedure for ultimate displacement is warranted.

This study shows that a high damping coefficient for the contact zone between the hammer and the RPC beam should be required in the impact response analysis. However, the size and geometry of the contact part of the hammer may strongly affect the damping coefficient for the local response, so that further research is required for a general determination of the damping coefficient.

6. Conclusions

Based on the results presented in this paper, the following conclusions can be drawn.

1. RPC beams subjected to impact loading show a type of ductile flexural tension failure with numerous fine cracks when no shear reinforcement is provided to the RPC beams.
2. The maximum midspan deflection of the RPC beam increases proportionally with increases in drop height.
3. Regardless of the loading type, such as static or impact, the degree of flexural damage to the RPC beam only depends on the maximum deformational response.
4. The two degrees of freedom mass-spring-damper system model was developed to represent the response of the RPC beam subjected to a drop hammer impact loading. The analytical results are in good agreement with the experimental results when high damping for the local response at the contact point is assumed.
5. The analytical results show that the maximum absorbed energy of the RPC beam corresponds to 82% to 86% of the input energy; thus 14% to 18% of the input energy is lost.

References

Fujikake, K., Uebayashi, K., Ohno, T., Shimoyama, Y. and Katagiri, M. (2002). "Dynamic properties of steel fiber reinforced mortar under high-rates of loadings and triaxial stress states." *In:* N. Jones, C. A. Brebbia, and A. M. Rajendran, Eds., *Proceedings of the 7th International Conference on Structures Under Shock and Impact, Montreal*, WIT Press, 437-446.

Fujikake, K., Senga, T., Ueda, N., Ohno, T. and Katagiri, M. (2006a). "Effects of strain rate on tensile behavior of reactive powder concrete." *Journal of Advanced Concrete Technology*, 4 (1), 79-84.

Fujikake, K., Senga, T., Ueda, N., Ohno, T. and Katagiri, M. (2006b). "Nonlinear analysis for reactive powder concrete beams under rapid flexural loadings." *Journal of Advanced Concrete Technology*, 4 (1), 85-97.

JSCE (1993). "*Impact Behavior and Design of Structures*." Structural Engineering Series 6. (in Japanese)

JSCE (2004). "*Practical Methods for Impact Test and Analysis*." Structural Engineering Series 15. (in Japanese)

Norwegian Defence Construction Service (1996). "*Precision Testing in Support of Computer Code Validation and Verification*." *In:* T. Krauthammer, A. Jenssen and M. Langseth, Eds., Workshop Report.

Ueda, N., Fujikake, K., Ohno, T. and Katagiri, M. (2005). "Dynamic flexural behaviors of RPC beams under high-rate loadings. [CD-ROM]" *In:* N. Banthia, T. Uomoto, A. Bentur, and S. P. Shah, Eds., *Proceedings of the 3rd International Conference on Construction Materials*, Vancouver, The University of British Columbia.